Crack Resistance Behavior of Polyvinylchloride

MINGCHENG CHE, WOLFGANG GRELLMANN, SABINE SEIDLER

Department of Materials Science, Martin-Luther University Halle-Wittenberg, D-06099 Halle (Saale), Germany

Received 13 July 1996; accepted 23 October 1996

ABSTRACT: The effects of specimen dimension (thickness, width) and specimen configuration (SENB, CT), as well as test conditions (crosshead speed, temperature), over a range of crosshead speeds from 0.01 to 100 mm/min and temperatures from −40 to 60°C, on the crack growth resistance behavior were investigated in a commercial amorphous thermoplastic polyvinylchloride (PVC) using the *J*-integral and crack opening displacement (COD) concepts. With the combined application of these two different fracture mechanics parameters, more detailed information on fracture processes can be obtained. The relationship between deformation mechanisms and fracture toughness was discussed through a comparative analysis of J versus Δa and COD versus Δa resistance curves. © 1997 John Wiley & Sons, Inc. J Appl Polym Sci **64:** 1079–1090, 1997

Key words: polyvinylchloride; crack resistance curve; specimen dimension and configuration; crosshead speed; temperature

INTRODUCTION

Fracture mechanics behavior of polymeric materials has been intensively researched during recent years.[1–8] However, the test results have not yet been fully understood. Furthermore, the practical applications of fracture mechanics values on structural integrity assessment are strongly restricted due to their limited transferability from specimens to components. Moreover, with the exception of the ESIS TC4 recommendation for plastics,[9] no standardized test procedures for tough polymeric materials exist to carry out fracture toughness testing; hence, those developed for metallic materials are simply adopted. All of these have induced great efforts to seek for geometry-independent fracture mechanics parameters.

Several fracture mechanics parameters have been proposed for the evaluation of the crack resistance behavior. Among these, the *J*-integral[1–3] and crack opening displacement (COD)[4] methods were mostly used to study polymeric materials that exhibit significant crack tip plastic deformations during the process of fracture. A combined application of the *J*-integral and COD concepts has been introduced by our working group on thermoplastics,[5] particle-reinforced composites,[6] and fiber-reinforced composites[7,8] under impact loading. *J*-integral describes the energy determined and COD describes the deformation determined fracture process. The combined application contributes to better understanding of the fracture behavior.

While the fracture mechanics behavior in brittle polymeric materials has been clearly studied using the linear elastic fracture mechanics (LEFM) theory, there is no established agreement with respect to the influence of specimen dimensions, specimen configurations, and test conditions on the crack resistance behavior in tough polymeric materials. In the present study, the influence of specimen dimension (specimen thickness, specimen width), configuration (compact tension (CT) and single edge notched bend (SENB)), and test conditions (crosshead speed and test temperature) on crack resistance behavior is examined in polyvinylchloride (PVC) under quasi-static loading. Both the *J*-integral and COD concepts were used. The specimen size criteria to construct valid crack

Correspondence to: W. Grellmann, Fax: (0049 3461) 462592 E-mail: w.gr@werkstoff.uni-halle.de

Table I Experimental Program: Specimen Dimensions, Geometries, and Loading Conditions

Experimental Program	Geometry	Temperature (°C)	Crosshead Speed (mm/min)	Thickness B (mm)	Width W (mm)	a_0/W
Thickness	CT	23	1	4, 6, 8, 10, 15, 20	40	0.55
Width	SENB	23	1	10	20–40	0.55
Geometry	CT, SENB	23	1	10	40	0.55
Crosshead speed	CT	23	0.01–100	10	40	0.55
Temperature	SENB	−40–60	1	10	20	0.55

resistance curves were checked, and the fracture behavior under different test conditions was examined.

EXPERIMENTAL

Material and Method

The experimental program is summarized in Table I. The effects of specimen dimensions (thickness and width) and specimen geometry (CT and SENB) were examined at room temperature and at a crosshead speed of 1 mm/min. The influence of crosshead speed was studied on CT specimens at room temperature, while SENB specimens were used to study the temperature effect. The ratio of the initial crack length a_0 to the specimen width W was $a_0/W = 0.55$ throughout the tests. In the tested PVC, the fracture toughness was found to be independent of specimen thickness when the specimen thickness $B \geq 10$ mm, as is presented in this article. In order to avoid the possible additional effects of specimen thickness, the 10 mm thick specimens were used to study the effect of the factors other than the specimen thickness.

Specimens were prepared directly from commercial extruded PVC sheets with the crack growth direction along the extrusion direction and precracked at room temperature with a flycutter. Subsequently, the notch was sharpened by sliding a razor blade across the machined notch tip, which had a tip radius of 0.2 μm. The usual multiple-specimen testing method was applied. Several identical specimens were loaded up to different displacements and then rapidly unloaded. After that, the specimens were cooled in liquid nitrogen and then broken at a high loading rate. Using a traveling microscope, stable crack extensions Δa were measured from the exposed fracture surfaces and determined from a nine-point average along the specimen thickness.

For the tests on CT specimens, a ZWICK Z020 testing machine was used. The load-line displacement Δ was measured with the help of a contactless laser scanner system (Fig. 1). The system was specially developed for polymeric materials and demonstrates various advantages compared to the conventional mechanical clip gauge systems. SENB specimens were tested on an INSTRON 4507 testing machine equipped with a temperature chamber. The ratio of the span to the specimen width s/W is 4. The load-line displacement was measured with an internal crosshead transducer of the testing machine, and indentation corrections were made to account for deformation due to roll indentation, penetration of the loading pins, etc., according to ESIS TC4.[9]

Tensile properties measurements were also performed on the same INSTRON testing machine at the corresponding crosshead speeds and test temperatures to determine Young's modulus E and yield strength σ_y.

Data Analysis Procedure and Construction of *R*-Curves

In the present study, toughness was measured by the two elastic-plastic fracture mechanics

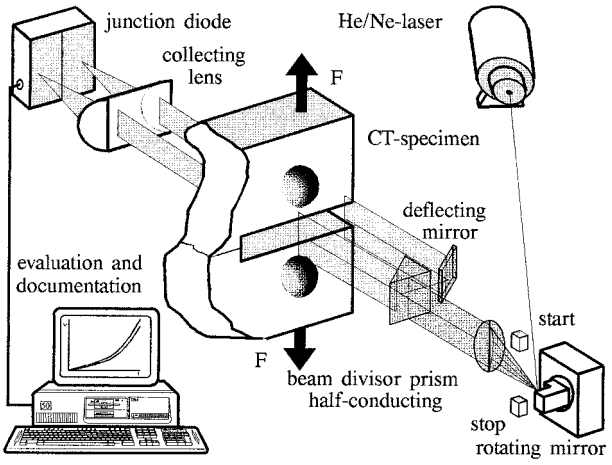

Figure 1 Laser double scanner system to measure load-line displacement and crack opening displacement on CT specimens.

(EPFM) parameters, the J-integral and COD. J-values were calculated with correction to the stable crack extension.[9]

$$J = J_0\left\{1 - \frac{(0.75\eta - 1)}{W - a_0}\right\} \quad (1)$$

with

$$J_0 = \frac{\eta U}{B(W - a_0)} \quad (2)$$

where

$\eta = 2 + 0.522a_0/W$ for CT specimens

and

$\eta = 2$ for SENB specimens with $s/W = 4$ (3)

where Δa is the actual crack extension at the relative loading level, and U is the area under the load versus load-line displacement curve.

The experimental COD was estimated by separating the COD into elastic and plastic components, as follows[10,11]:

$$\delta = \delta_{el} + \delta_{pl} \quad (4)$$

with

$$\delta_{el} = \frac{K^2(1 - \nu^2)}{2E\sigma_y} \quad (5)$$

where K is stress intensity factor, $K = \frac{F}{B\sqrt{W}} f(a_0/W)$, F is the actual load, and $f(a_0/W)$ is the stress intensity function.[11]

For the CT specimen, the δ_{pl} was determined from the plastic component of the mouth opening displacement v_{pl}[10,11]:

$$\delta_{pl} = \frac{r_{pl}[W - (a_0 + \Delta a)] + \Delta a}{r_{pl}[W - (a_0 + \Delta a)] + (a_0 + \Delta a) + z} v_{pl} \quad (6)$$

where v_{pl} is the plastic component of the mouth opening displacement, and z is the distance of the knife edge from the load line. For the SENB specimen, the δ_{pl} was inferred directly from the load F versus the load-line displacement Δ curve based on the method from Anderson, McHenry, and Dawes[12] using the stable crack growth correction, as follows:

$$\delta_{pl} = \frac{4\Delta_{pl}}{s - \Delta_{pl}/4}\{r_{pl}[W - (a_0 + \Delta a)] + \Delta a\} \quad (7)$$

where Δ_{pl} is the plastic component of the load-line displacement Δ on a SENB specimen, and s is the support span. The relationship was derived by assuming that the SENB specimen deforms in pure bending about a hinge point at a distance of $r_{pl}[W - (a_0 + \Delta a)]$ in front of the actual crack tip; the specimen halves are assumed to remain rigid.

According to ASTM 1290,[11] the plastic rotational factor r_{pl} is specified as

$$r_{pl} = 0.4(1 + \alpha) \quad (8)$$

with

$$\alpha = 2\sqrt{[a_0/(W - a_0)]^2 + a_0/(W - a_0) + 0.5} - 2[a_0/(W - a_0) + 0.5] \quad (8a)$$

for a CT specimen, and

$$\alpha = 0.1 \quad (8b)$$

for a SENB specimen.

To construct valid R-curves, only the data points within the window defined by the exclusion lines Δa_{min}, Δa_{max}, and J_{max} or δ_{max} were used

$$\Delta a_{min} = 0.05 \text{ mm}, \Delta a_{max} = 0.1(W - a_0), \text{ and } J_{max} = \text{smaller of } B\sigma_y/20 \text{ or } (W - a_0)\sigma_y/20 \quad (9a)$$

by construction of J-R curves,[9] and

$$\Delta a_{min} = 0.10 \text{ mm}, \Delta a_{max} = 0.1(W - a_0), \text{ and } \delta_{max} = \text{smaller of } B/50 \text{ or } (W - a_0)/50 \quad (9b)$$

by construction of δ-R curves.[10] Δa_{min} is only an artifact to avoid subjective measurement error, and that proposed for J-integral $\Delta a_{min} = 0.05$ mm can be also accepted for COD. The factor 50 in δ_{max} from ESIS P2-91[10] seems to be too great for the amorphous PVC. In reference with J_{max} from ESIS TC4,[9] we suggest 20 instead of 50. This suggestion is supported by our own experimental results in the present study. R-curves were then

constructed by plotting values of J-integral or COD as a function of crack extension Δa and a fit curve was drawn using a simple power law of the form

$$J \text{ or } \delta = \mathrm{X}\Delta a^{\mathrm{Y}} \tag{10}$$

where X and Y are constants. In accordance with ESIS TC4,[9] the crack initiation toughness J_{IC} was evaluated at a stable crack extension of 0.2 mm, denoted as $J_{0.2}$. Similarly, $\delta_{0.2}$ was determined as the crack initiation COD value. The validity of the initiation values was checked with the specimen size requirements.

Whereas initiation toughness provides information about the crack initiation resistance, the slope of the R-curves is indicative of the resistance against the stable crack growth.[13] The slope is quantified by a dimensionless tearing modulus at a prescribed amount of stable crack extension, denoted as T_J for J resistance curves,

$$T_J = \frac{E}{\sigma_y^2} \cdot \frac{dJ}{d\Delta a} \tag{11a}$$

and T_δ for δ resistance curves,

$$T_\delta = \frac{E}{\sigma_y} \cdot \frac{d\delta}{d\Delta a}\,. \tag{11b}$$

In an analogy to the determination of the crack initiation values, the tearing moduli were determined at a stable crack growth of $\Delta a = 0.2$ mm and were signed as $T_{J_{0.2}}$ for J resistance curves and $T_{\delta_{0.2}}$ for δ resistance curves, respectively.

RESULTS AND DISCUSSION

The results and discussion will be presented in the following six sections: 1) tensile properties, 2) effect of specimen thickness, 3) effect of specimen width, 4) effect of specimen configuration, 5) effect of crosshead speed, and 6) effect of test temperature.

Tensile Properties

The Young's modulus E and the yield strength σ_y are shown in Figure 2(a) as a function of crosshead speed at room temperature and in Figure 2(b) as a function of test temperature at a crosshead speed of 1 mm/min. Both of them increase with increasing crosshead speed. Although the yield strength decreases linearly with increasing temperature, the Young's modulus decreases first with increasing temperature, then afterwards stays relatively constant between −20 and 40°C, then decreases again.

Effect of Specimen Thickness

Figure 3(a) and (b) show the J-R and δ-R curves in dependence on the specimen thickness ranging from 4 to 20 mm at a crosshead speed of 1 mm/min at room temperature. By strictly following the procedure proposed by ESIS TC4,[9] only one valid J-value can be obtained on specimens with $B = 4$ mm. For purposes of comparison, the $J_{\max}$ restriction condition was neglected on these specimens with $B = 4$ mm, and their fracture mechanics parameters are also presented in Figure 4(a), together with the other valid ones. The thickness dependencies of initiation values and tearing moduli based on the J-integral [Fig. 4(a)], as well as the COD concept [Fig. 4(b)], show a transition region from a plane-stress state to a plane-strain state around $B = 6$ mm, where local maxima of fracture mechanics parameters occur. With increasing thickness, the thickness-independent fracture mechanics material constants are reached. The critical minimal specimen thickness was determined to be 10 mm in the tested PVC, and the thickness−independent initiation values are $J_{0.2} = 8.3$ N/mm and $\delta_{0.2} = 0.13$ mm. A similar critical minimal specimen thickness was obtained by Huang.[14] The specimen size requirements for the initiation values were satisfied.

Effect of Specimen Width

The load-deflection curves for the SENB specimens with specimen width of 20 and 40 mm are compared in Figure 5, with data points indicating the stable crack extensions from the differently loaded identical specimens. As can be seen from the J versus Δa and δ versus Δa curves in Figure 6, the specimen width has no influence on the resistance curves. However, the restriction condition for $\delta_{\max}$ (eq. 9b) is too severe for the tested polymeric material PVC. Instead of 50, we suggested 20, based on our experimental results.[15]

Effect of Specimen Configuration

The effect of specimen configuration on resistance behavior was studied using SENB and CT speci-

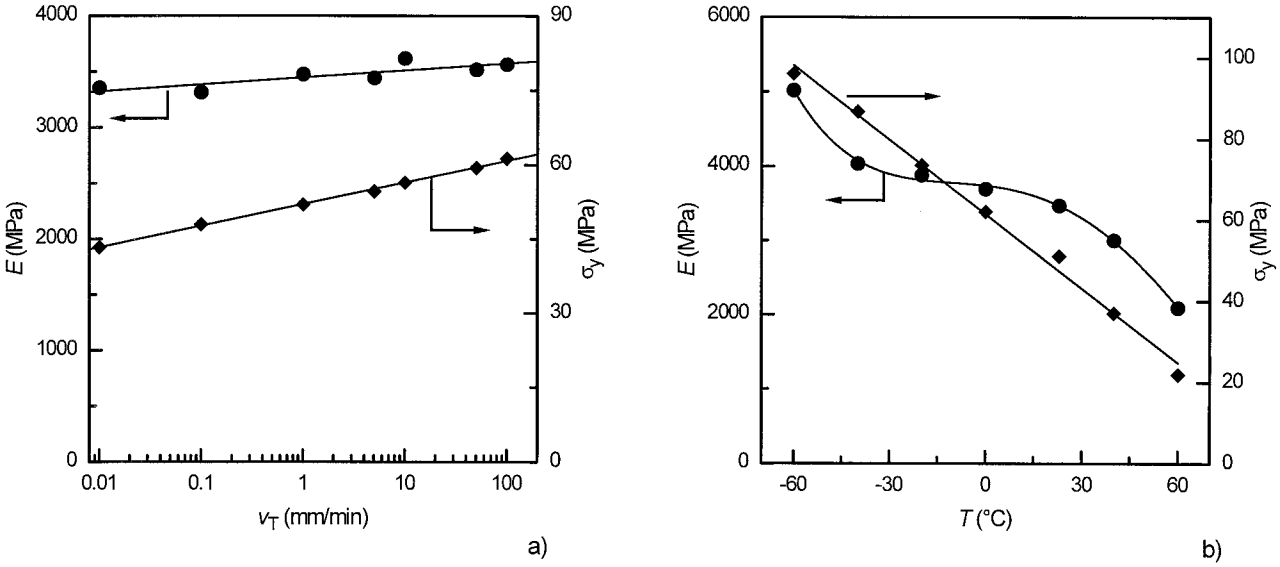

Figure 2 Tensile properties in dependence of (a) crosshead speed and (b) test temperature.

mens at room temperature and at a crosshead speed of 1 mm/min. Load versus load-line displacement curves are shown in Figure 7. The maximum load F_{max} on the SENB specimen is the same as on the CT specimen, but at a greater load-line displacement, and the whole F versus Δ curve of the SENB specimen seems to be elongated from that of the CT specimen along the load-line displacement axis. However, the δ versus Δa curves are independent of specimen configuration [Fig. 8(a)], and the crack resistance in terms of J versus Δa on the SENB specimens is somewhat greater than that of the CT specimens, i.e., with a higher $J_{0.2}$ value and steeper slope [Fig. 8(b)]. Hashemi and Williams[16] have used J method to investigate the influence of specimen configuration in different polymeric materials. A similar effect was found in PVC and rubber-modified polyvinylchloride (PVCR), as presented here. But in several other researched polymers, such as low-density polyethylene (LDPE), medium-high-density polyethylene (MDPE), high-density polyeth-

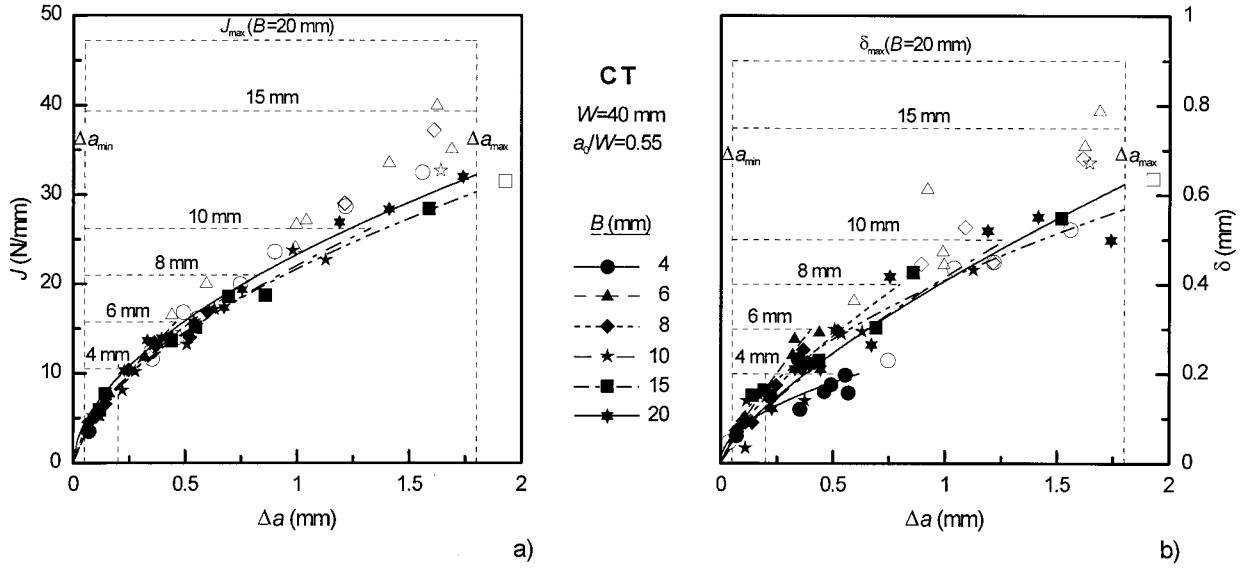

Figure 3 Effects of specimen thickness on (a) J versus Δa curves and (b) δ versus Δa curves (●, ▲, ◆, ★, ■, ✶: valid points. ○, △, ◇, ☆, □, ✲: invalid points).

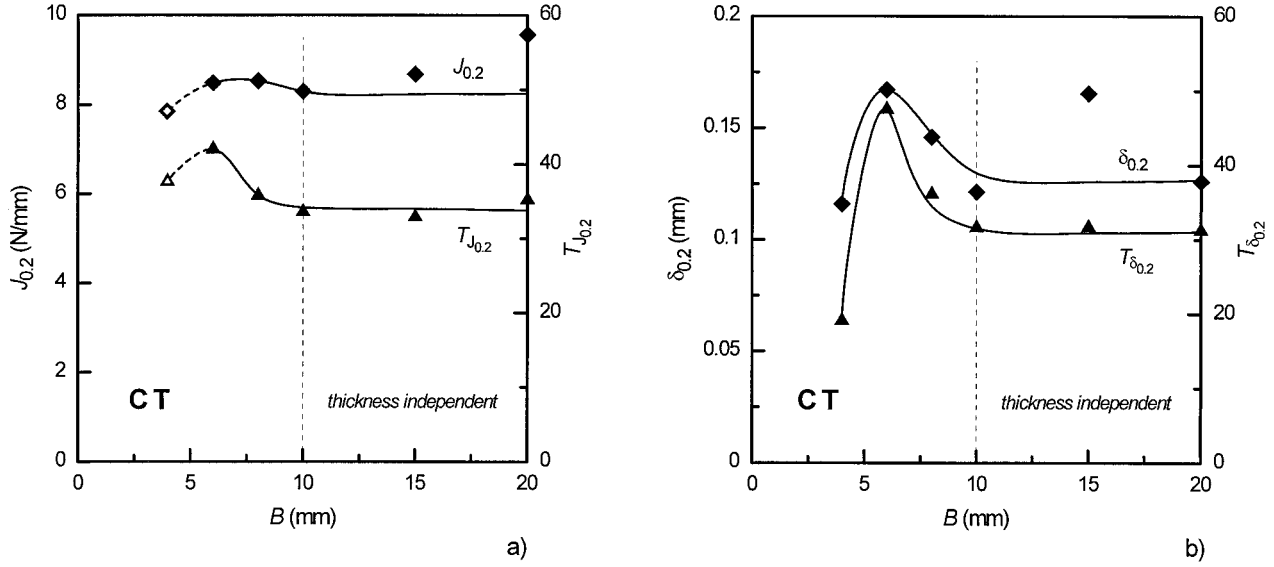

Figure 4 Dependence of crack resistance on specimen thickness using the (a) J and (b) COD method.

ylene (HDPE), and polystyrene (PS), no influence of specimen geometry was observed. It seems that the effect of specimen configuration on crack resistance behavior is coupled with the material behavior.

The measured J is a global energy input into the cracked specimens and should be influenced by the deformation behavior of the crack tip zone. The difference in crack tip constraint contributes to the effect of the specimen configuration on the J versus Δa curves. With the help of the finite element method, it has been numerically demonstrated that by using the Rice–Drugan–Sham (RDS) stable crack growth criterion[17] with only

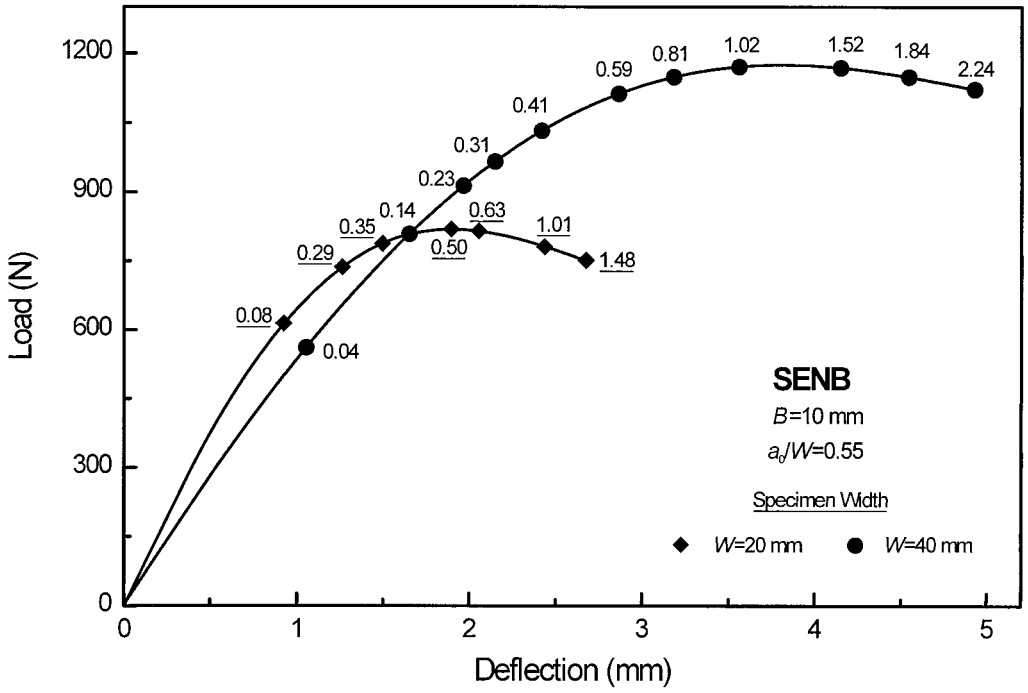

Figure 5 Comparison of load versus deflection curves on SENB specimens with different specimen widths (v_T = 1 mm/min).

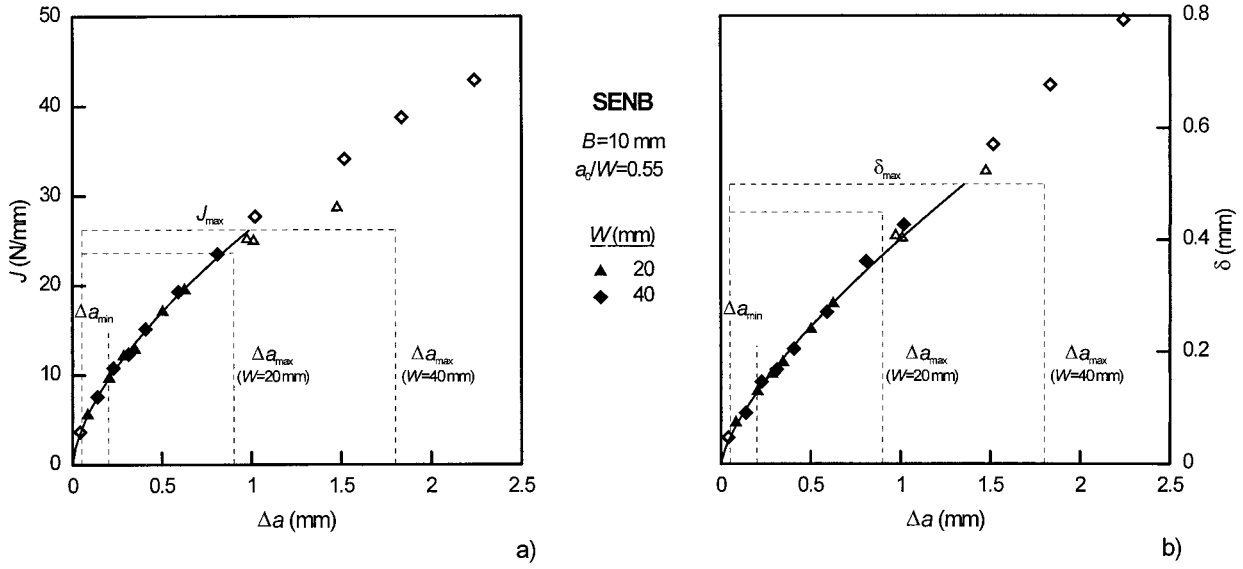

Figure 6 Effects of specimen width on (a) J versus Δa and (b) δ versus Δa curves (SENB, v_T = 1 mm/min).

a single value of crack tip opening angle CTOA $\approx$ 40 degrees at a distance of 0.1 mm behind the actual crack tip, the configuration-independent δ versus Δa curves and the configuration-dependent J versus Δa curves can be numerically well simulated in the mean time.[18] In view of the configuration effects, the application of the local fracture mechanics parameter COD is more appropriate than using the global J integral.

Effect of Crosshead Speed

Time-dependent fracture behavior is not unexpected as the tensile properties show [Fig. 2(a)]. In the literature, a different time-dependent fracture behavior was reported by using the J method. While no influence of loading rates was observed,[2,19] a reduction,[20] as well as an increase of crack resistance,[21] was also found with increasing loading rates.

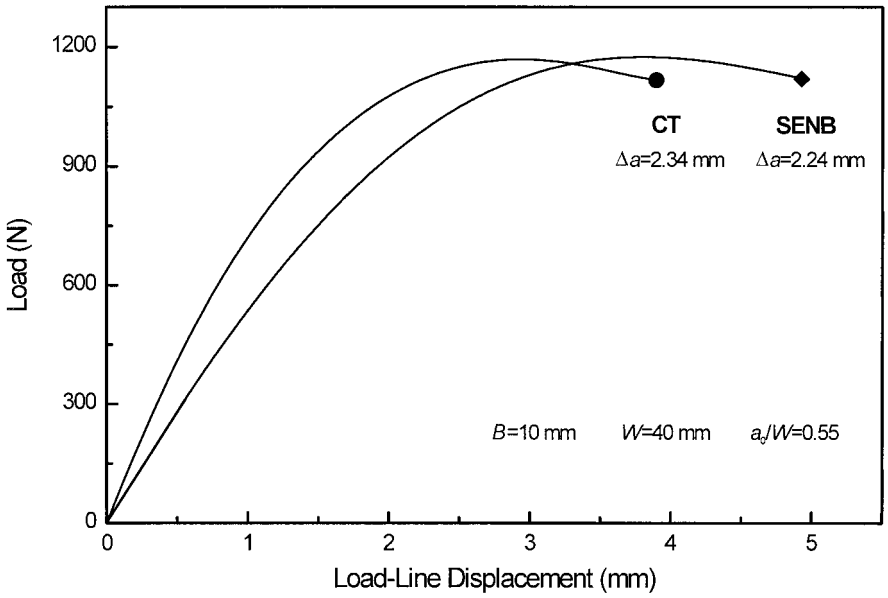

Figure 7 Comparison of load versus load-line displacement curves on CT and SENB specimens.

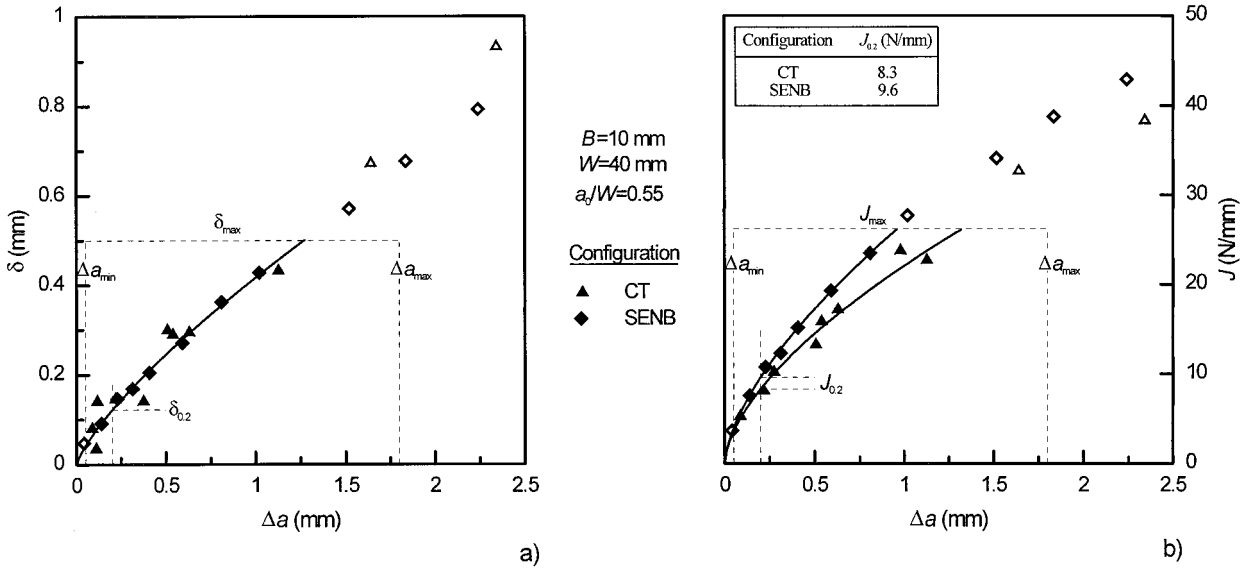

Figure 8 Effects of specimen configurations on (a) δ versus Δa curves and (b) J versus Δa curves.

The J versus Δa and δ versus Δa curves are presented in Figure 9, and the initiation values and the tearing moduli are shown in Figure 10 as a function of the crosshead speed. The $J_{0.2}$ values show a two-range behavior, and the local maximum occurs at v_T = 5 mm/min [Fig. 10(a)]; while the tearing modulus $T_{J_{0.2}}$ remains constant up to v_T = 5 mm/min, then decreases with increasing loading rates [Fig. 10(a)]. Using the COD concept [Fig. 10(b)], the initiation value $\delta_{0.2}$ remains constant until v_T = 5 mm/min is reached, then decreases with increasing crosshead speeds. The tearing modulus $T_{\delta_{0.2}}$ behaves approximately in the same way. From Figure 10, it can be concluded that for the tested PVC, the time-dependent crack initiation resistance should be evaluated by using both $J_{0.2}$ and $\delta_{0.2}$ values, while the time-dependent crack growth resistance can be well characterized by either $T_{J_{0.2}}$ or $T_{\delta_{0.2}}$.

Moreover, the combined application of these two fracture mechanics parameters contributes to a better understanding of the time-dependent resistance behavior and of the micromechanical fracture processes. At lower crosshead speeds, there is enough time to develop the relaxation processes, and the crack tip blunting will be well formed. Hence, the local crack tip fracture is induced due to plasticity exhaustion, and the initiation δ-value is then a material constant. With the constant initiation δ-value, the time dependence of the J_{IC} can be then predicted, as follows[22]:

$$J_{IC} \propto (\dot{\varepsilon})^m \tag{12}$$

where m is the exponent in the dependence of the yield strength on the strain rate.

The two-range behavior of the $J_{0.2}$ values is described under consideration of this fracture model (eq. 12) in Table II. The experimentally determined exponent b = 0.03 at lower crosshead speeds $v_T \leq$ 5 mm/min (Table II) agreed well with that from the dependence of the yield strength on the strain rate, m = 0.04 [Fig. 2(a)].

At higher crosshead speeds, the plastic blunting process would be strongly reduced, and the relaxation capacity cannot be well exploited, which leads to a strong decrease of the crack resistance with further increase of the crosshead speed. This effect in the PVC is enhanced due to its greater notch sensibility. At very high crosshead speeds, the additional influence of the local adiabatic heating can exist.

Effect of Test Temperature

Typical load-deflection curves at different temperatures are shown in Figure 11, where the data represent the stable crack extensions at the corresponding test termination. Increasing temperature decreases the slope of the load versus load-deflection curves. To produce a same stable crack size, more deflection should be used at higher temperature. However, the maximum load F_{max}

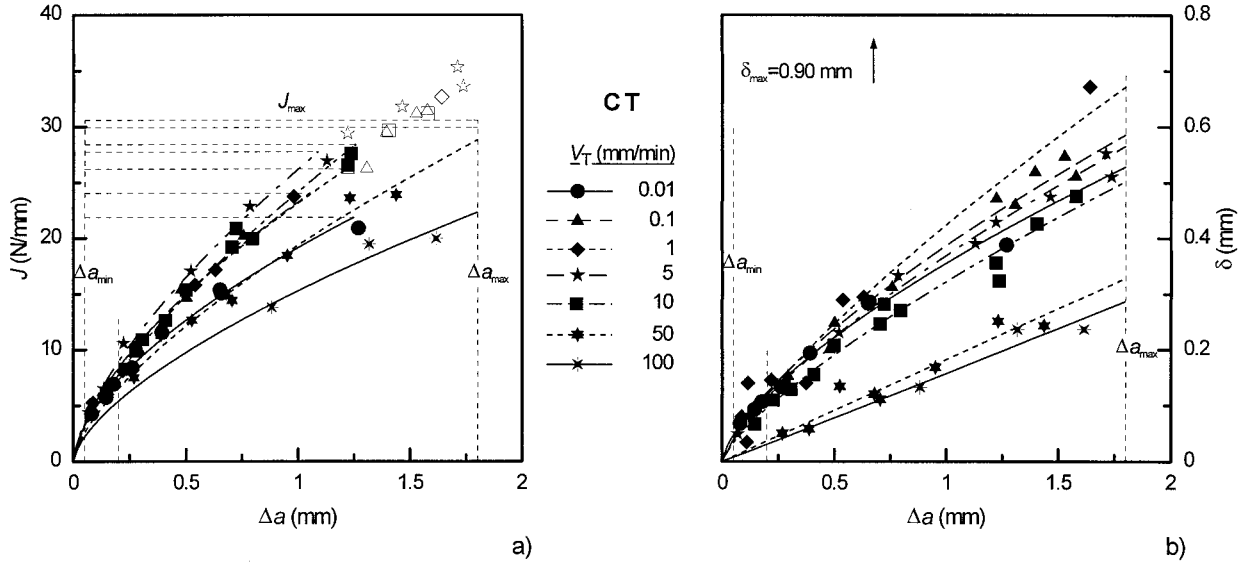

Figure 9 (a) J versus Δa curves and (b) δ versus Δa curves of CT specimens at different crosshead speeds.

showed a maximum value at $T = 23°C$, and the crack extension at F_{max} is strongly dependent on the test temperature.

The J-R and δ-R curves are shown in Figure 12(a) and (b) as a function of test temperature. If the procedures recommended in ESIS TC4[9] and ESIS P2-91[10] are strictly followed, there is an insufficient number of valid data points to construct J-R and δ-R curves. However, for purposes of comparison, the validity restrictions of J_{max} and δ_{max} are not considered, and only the restrictions Δa_{min} and Δa_{max} are taken into consideration. The values of $J_{0.2}$ and $\delta_{0.2}$, as well as their corresponding tearing moduli, are plotted as a function of test temperature in Figure 13(a) and (b). Whereas the $J_{0.2}$ and $T_{J_{0.2}}$ values show a different behavior in dependence on temperature, the $\delta_{0.2}$ and $T_{\delta_{0.2}}$ values show similar behavior. As can be obviously seen, the deformation relevant fracture mechanics parameter COD only represents the temperature dependence of the crack tip deformability; therefore, it is not appropriate to use a single parameter COD to evaluate the temperature effect on the crack initiation resistance. In

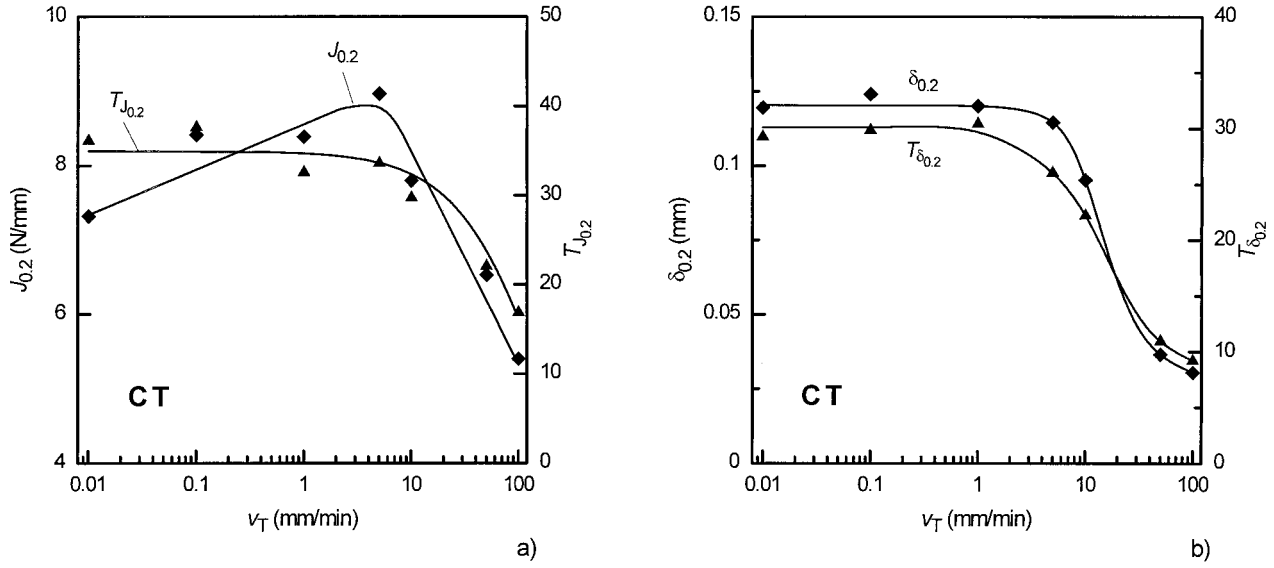

Figure 10 Influence of crosshead speed on fracture mechanics parameters: (a) $J_{0.2}$ and $T_{J_{0.2}}$ and (b) $\delta_{0.2}$ and $T_{\delta_{0.2}}$.

Table II Power Law Fitting of the Crack Initiation Values $J_{0.2}$ to $\dot{\varepsilon}$ in the Two Loading Rate Ranges

Rate Range (mm/min)	$J_{0.2} = a\dot{\varepsilon}^b$		Correlation Coefficient (R^2)
	a	b	
0.01–5	10.5	0.03	0.86
5–100	3.7	−0.15	0.97

contrast, the elastic-plastic energy-relevant J integral concept, including loading capacity and crack tip deformability, seems more suitable. As observed in the time-dependent crack resistance behavior, the tearing moduli of these two parameters also show similar temperature dependencies of the resistance against crack stable growth (Fig. 13). Similarly, we can conclude that only with the combined applications of these two EPFM parameters (J integral and COD), the temperature-dependent crack initiation behavior can be well characterized, and the temperature-dependent crack growth behavior can already be well described by only using the tearing modulus of either the J integral or COD.

The local maximum of the $J_{0.2}$ values occurs at nearly 23°C. The temperature location of this peak can not be attributed to the β-relaxation process, which occurs around −30°C.[23] This local maximum of the energy relevant $J_{0.2}$ values is attributed to the temperature dependence of the fracture stress because no respective local maximum was observed in the temperature dependence of the crack tip deformation [Fig. 13(b)]. The steady increase of $T_{J_{0.2}}$ and $T_{\delta_{0.2}}$ with increasing temperature results from the increasing slope of the J versus Δa curves, and of the δ versus Δa curves and the temperature dependence of the elastic properties, respectively [Fig. 2(b)]. This temperature dependence is different to that found by Johnson and Radon[24] over a wide range of strain rates using the K concept. A weak maximum in the K_{IC} versus temperature was observed at a temperature below the glass transition temperature T_g, the location of which varied with testing speed and was moved to higher temperatures with increasing testing speed. The difference between slow bend and impact data may be partly due to increased amounts of crazing in the former case. The fracture mode becomes more and more unstable with decreasing temperature.

Quite different results were observed by Hashemi and Williams[2] on PVC in a temperature range between −20 and 20°C, where J_{IC} decreased with increasing test temperature and

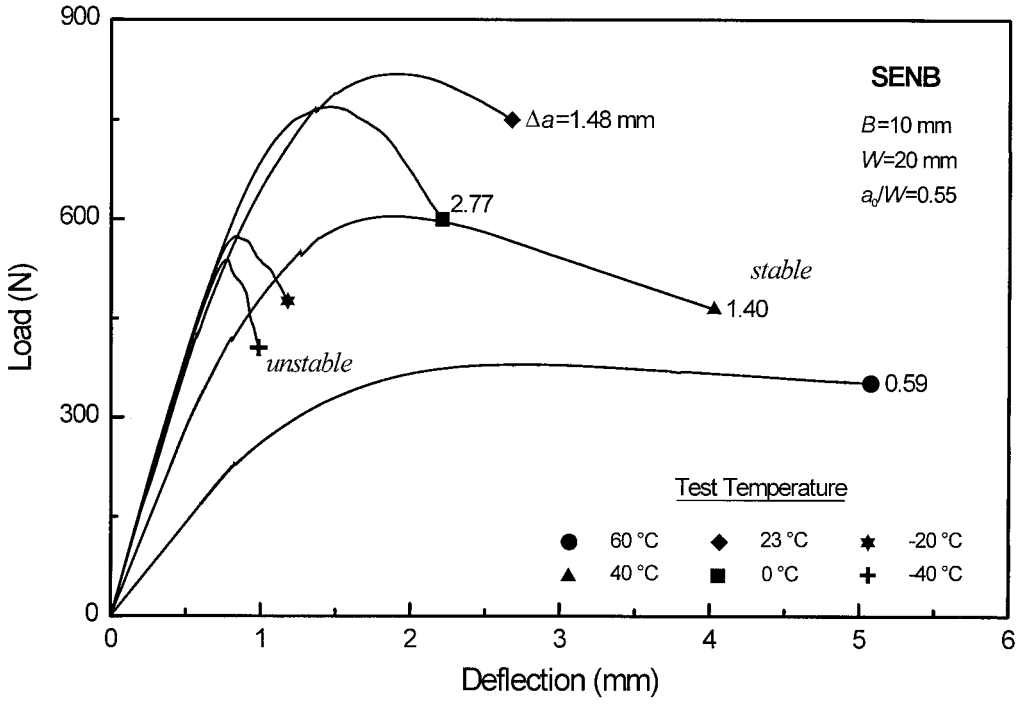

Figure 11 Load versus deflection curves as a function of test temperature (SENB, v_T = 1 mm/min).

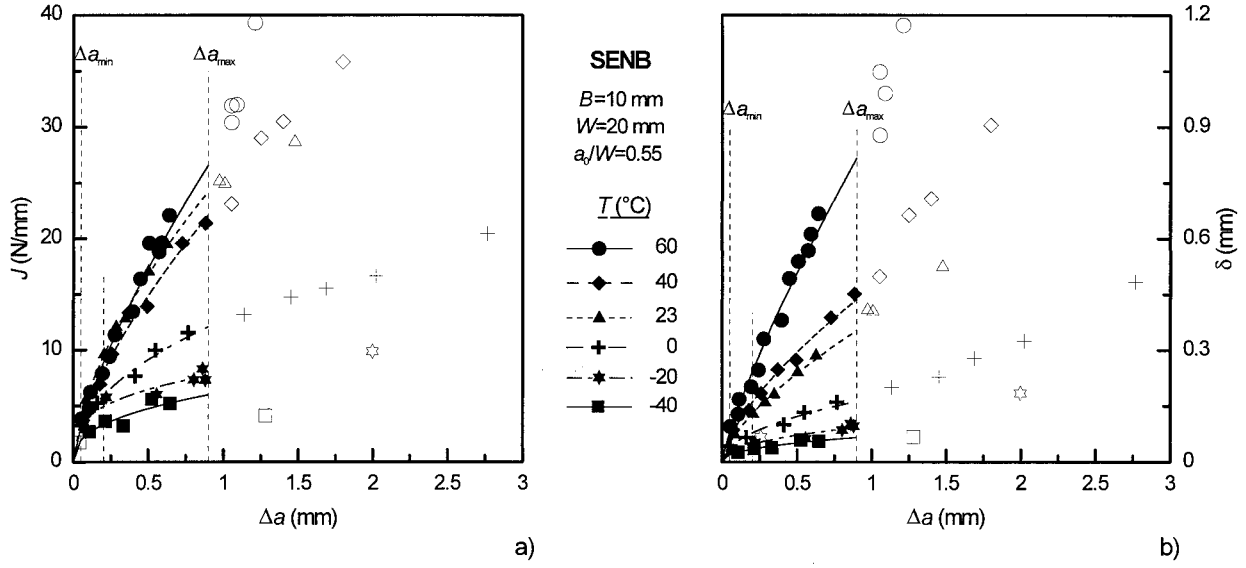

Figure 12 (a) J versus Δa curves and (b) δ versus Δa curves at different test temperatures.

ASTM E813-81[25] was followed to determine J_{IC}. The toughness is a complex property and depends on various different parameters. It can be seen, especially, that the temperature effect depends on materials behavior and test conditions. More detailed research on the relationship between fracture toughness and other mechanical properties, as well as the micromechanical mechanisms, are required under wider test conditions and in a wider materials spectrum.

CONCLUSIONS

With the combined application of the J-integral and COD concepts, the fracture processes in dependence on the specimen dimension, configuration, and test conditions have been examined. The following conclusions can be drawn.

1. The critical specimen thickness for the specimen thickness-independent fracture

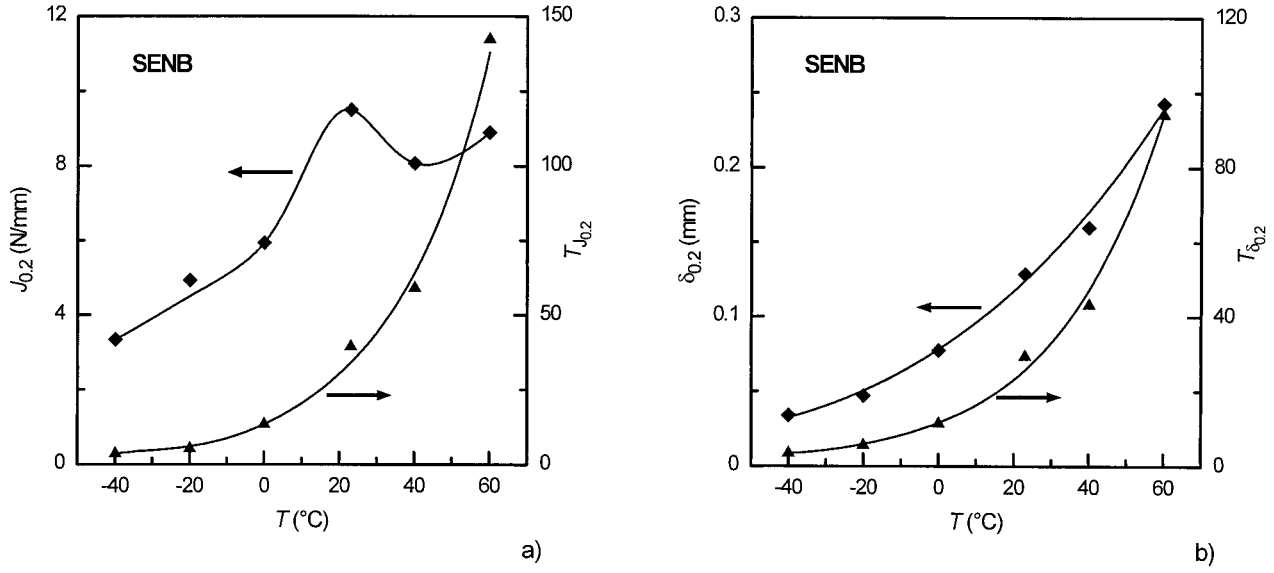

Figure 13 Temperature effect on fracture mechanics parameters: (a) $J_{0.2}$ and $T_{J_{0.2}}$ and (b) $\delta_{0.2}$ and $T_{\delta_{0.2}}$.

toughness is found to be 10 mm, and no effect of the specimen width occurs.

2. The crack resistance, in terms of δ versus Δa, is independent of the specimen configuration (SENB and CT); while the crack initiation resistance $J_{0.2}$ on the SENB specimen is somewhat greater, and the slope of the J versus Δa curve is steeper than that on the CT specimen.
3. The tested PVC shows a strong time-dependent crack resistance behavior. In the range of crosshead speeds from 0.01 to 5 mm/min, the crack initiation J value increases with increasing crosshead speed, while the crack initiation crack opening displacement remains constant. The time dependence of the crack initiation J values can be confirmed by using the local fracture criterion with a constant critical COD. With further increase of crosshead speed, the $J_{0.2}$ and $\delta_{0.2}$ values decrease, which results from the reduction of the plastic blunting at the crack tip. However, the tearing moduli $T_{J_{0.2}}$ and $T_{\delta_{0.2}}$ remain unchanged up to v_T = 5 mm/min and then decrease steadily with increasing crosshead speed.
4. Similarly, a strong temperature effect is observed. The crack initiation values in terms of the J integral show a maximum value at T = 23°C, while the $\delta_{0.2}$ values, as well as the tearing moduli either in terms of the J integral or of the COD concept, increase with increasing test temperature.

REFERENCES

1. M. K. V. Chan and J. G. Williams, *Int. J. Fract.,* **23,** 145 (1983).
2. S. Hashemi and J. G. Williams, *Polym. Eng. Sci.,* **28,** 760 (1986).
3. I. Narisawa and M. T. Takemori, *Polym. Eng. Sci.,* **29,** 671 (1989).
4. X. Lu and N. Brown, *J. Mat. Sci.,* **21,** 4081 (1986).
5. W. Grellmann and S. Seidler, in *Reliability and Structural Integrity of Advanced Materials,* Vol. I, S. Sedmak, Ed., ESIS, Varna, 1992, p. 202.
6. J. Bohse, W. Grellmann, and S. Seidler, *J. Mat. Sci.,* **26,** 6715 (1991).
7. W. Grellmann, S. Seidler, and E. Nezbedova, *Makromol. Chem., Macromol. Symp.,* **41,** 195 (1991).
8. W. Grellmann and S. Seidler, *J. Polym. Eng.,* **11,** 71 (1992).
9. Standard Draft ESIS TC4 Test Protocol, *A Testing Protocol for Conducting J-Crack Growth Resistance Curve Tests on Plastics,* European Structural Integrity Society, 1991.
10. Standard Draft ESIS P2-91, *Procedure for Determining the Fracture Behaviour of Materials,* European Structural Integrity Society, 1991.
11. ASTM E1290-93, *Standard Test Method for Crack-Tip Opening Displacement (CTOD) Fracture Toughness Measurement,* American Society for Testing and Materials, Philadelphia, 1993.
12. T. L. Anderson, H. I. McHenry, and M. G. Dawes, in *Elastic-Plastic Fracture Test Method: The User's Experience, ASTM STP 856,* E. T. Wessel and F. J. Loss, Eds., Philadelphia, 1985, p. 210.
13. T. L. Anderson, *Fracture Mechanics Fundamentals and Applications,* 2nd ed., CRC Press, Boca Raton, Florida, 1995.
14. D. D. Huang, in *Advances in Fracture Research, ICF 7,* K. Salama and K. Ravi-Chaudar, Eds., University of Houston, 1989, p. 2725.
15. W. Grellmann and S. Seidler, *Int. J. Fract.,* **68,** R19 (1994).
16. S. Hashemi and J. G. Williams, *Plas. Rub. Proc. Appl.,* **6,** 363 (1986).
17. J. R. Rice, W. J. Drugan, and T. L. Sham, *ASTM STP 700,* Philadelphia, 1980, p. 189.
18. M. Che and W. Grellmann, *Eng. Fract. Mech.,* to appear.
19. C. R. Bernal and P. M. Frontini, *Polym. Testing,* **11,** 271 (1992).
20. D. D. Huang and J. G. Williams, *J. Mat. Sci.,* **22,** 2503 (1987).
21. R. E. Jones and W. L. Bradley, in *Nonlinear Fracture Mechanics: Vol. I, Time-Dependent Fracture, ASTM STP 995,* A. Saxena, J. D. Landes, and J. L. Bassani, Eds., Philadelphia, 1989, p. 447.
22. J. G. Williams, *Fracture Mechanics of Polymers,* Halsted Press, Wiley, New York, 1984.
23. F. Ramsteiner, *Kunststoffe,* **73,** 148 (1983).
24. F. A. Johnson and J. C. Radon, *J. Polym. Sci.,* **13,** 495 (1975).
25. ASTM E813-81, *The Determination of J_{IC}: A Measure of Fracture Toughness,* American Society for Testing and Materials, Philadelphia, 1981.